Balancing Power Absorption and Structural Loading for a Novel Fixed-Bottom Wave Energy Converter with Nonideal Power Take-Off in Regular Waves

Nathan Tom*
NREL[x]
Boulder, CO, USA

Yi-Hsiang Yu
NREL
Boulder, CO, USA

Alan Wright
NREL
Boulder, CO, USA

*Corresponding author: nathan.tom@nrel.gov
[x]National Renewable Energy Laboratory (NREL)

1. INTRODUCTION

The control of ocean energy harvesting devices has received significant attention in the marine engineering community and is considered necessary for economical ocean deployment. Several types of control methodologies have been previously proposed, such as complex conjugate [1], latching [2], and declutching. In recent years, the control of wave energy converters (WECs) using state-constrained optimization [3] has gained traction in the research community. The optimization has been performed using the calculus of variations [3], model predictive control [4], and pseudo-spectral methods [5]. These control strategies have been shown to be successful in maximizing power absorption but often neglect considerations for the peak forces, torques, and fatigue damage accumulation [6]. The next-generation WEC technologies will need to develop advanced feed-forward control methods and/or structures that adapt device performance to maximize energy generation in low-to-moderate sea states and begin shedding hydrodynamic loads with increasing wave height to maintain a high capacity factor. With this focus, a novel WEC concept that combines an oscillating surge wave energy converter (OSWEC) with control surfaces [7] has been developed at the National Renewable Energy Laboratory. The novel OSWEC has had its main body replaced by a set of rotatable flaps that provides control over the hydrodynamic properties, which is in contrast to traditional nearshore OSWEC designs [8]. In addition to the variable geometry concept, researchers have been developing control strategies that attempt to balance the power-to-load ratio of a WEC by penalizing the power-take-off (PTO) control and structural loads [4]. The controller must now balance opposing terms in an effort to obtain the greatest gains in absorbed power while allowing the smallest loads on the WEC structure. In this work, the net power delivered to the grid from a nonideal PTO is introduced followed by a review of the pseudo-spectral control (PSC) theory. A power-to-load ratio, used to evaluate the pseudo-spectral controller performance, is discussed, and the results obtained from optimizing a multiterm objective function are compared against results obtained from maximizing the net output power to the grid. Simulation results are then presented for four different OSWEC geometries to highlight the potential of combing both geometry and PTO control to maximize power while minimizing loads.

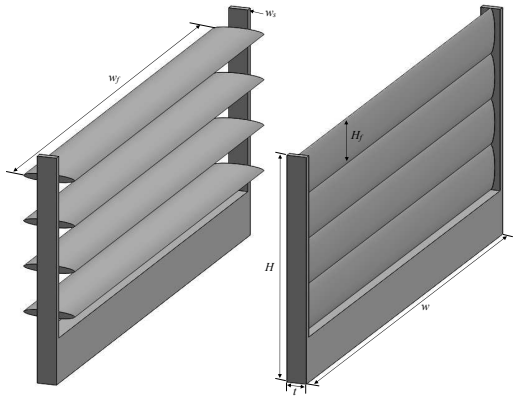

Figure 1: Solidworks rendering of the OSWEC. (Left) Perspective view of the fully open configuration (four flaps) and (right) perspective view of the fully closed configuration (zero flaps).

2. HYDRODYNAMIC MODELING

As described in a previous study [7], the main body of the novel OSWEC has been replaced with a set of identical flaps that may rotate about their center axis (see Fig. 1). However, for this investigation, the flaps were placed in either the fully closed (vertical) or open configurations (horizontal). The flaps may be opened independently but will only be allowed to open in descending order starting with the top flap located closest to the free surface. Therefore, no geometry is modeled

Table 1: Geometric Dimensions of the OSWEC

Water Depth, h, 10 m	Flap Minor Axis, t_f, 1/3 m
Height, H, 10 m	Flap Major Axis, H_f, 2 m
Thickness, t, 3/4 m	Support Width, w_s, 1/4 m
Width, w, 20 m	Center of Gravity, r_g, 3.97 m
Flap Width, w_f, 19.5 m	Inertia, I_{55}, 904.4 kg·m^2
Volume, $\forall$, 72 m^3	Mass, m, 36 t

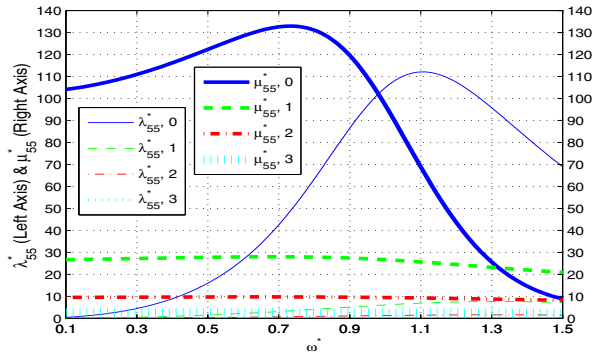

(a) $\omega^* = \omega\sqrt{h/g},\ \mu^*_{55} = \mu_{55}/I_{55},\ \lambda^*_{55} = \lambda_{55}/\omega I_{55}$

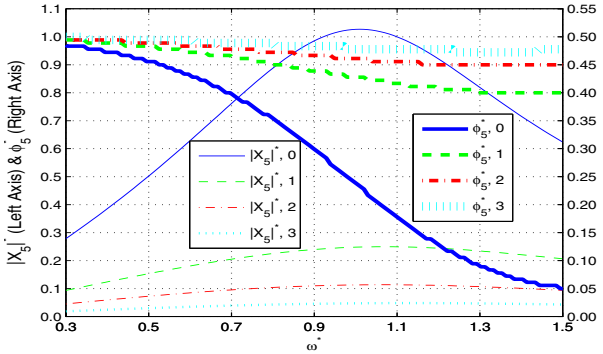

(b) $\omega^* = \omega\sqrt{h/g},\ X^*_5 = X_5/\rho g h^2 w,\ \phi^*_5 = \phi_5/\pi$

Figure 2: Nondimensional hydrodynamic radiation and wave excitation coefficients. The numbers in the legend correspond to the zero-flap, one-flap, two-flap, and three-flap open geometry.

that consists of a closed flap between two open flaps. The structural mass is assumed to be evenly distributed and the structural mass density (ρ_m) was set to half the fluid density (ρ). Therefore, the center of gravity will be equal to the center of buoyancy. The hydrodynamic coefficients were obtained from WAMIT version 7.2, and the hydrodynamic coefficients have been plotted in Fig. 2.

3. MAX POWER UNDER CONSTRAINTS

The maximum time-averaged power (TAP) (P_T) absorbed by a PTO under pitch displacement amplitude constraints, while assuming sinusoidal motion, was explored in [9], which provides the following expression

$$P_T = \begin{cases} \frac{1}{8}A^2|X_5|^2/\lambda_{55} & \delta > 1 \\ \frac{1}{2}A|X_5|\omega|\xi_5|_{max} - \lambda_{55}\omega^2|\xi_5|^2_{max} & \delta < 1 \end{cases} \quad (1)$$

where $|\xi_5|_{max}$ is the max pitch angular displacement, A is the wave amplitude, X_5 is the complex pitch wave-exciting torque per unit amplitude wave, λ_{55} is the radiation wave damping, and ω is the wave angular frequency. The term δ is the ratio between the constrained-to-optimal pitch angular velocity given by

$$\delta = \frac{\omega|\xi_5|_{max}}{A}\frac{2\lambda_{55}}{|X_5|} \quad (2)$$

Maximizing power absorption requires the linear PTO spring, C_g, and damping, λ_g, coefficients to be

$$\begin{aligned} \lambda_g &= \begin{cases} \lambda_{55} & , \ \delta > 1 \\ \frac{A|X_5|}{\omega|\xi_5|_{max}} - \lambda_{55} & , \ \delta < 1 \end{cases} \\ C_g &= -\left[C_{55} - \omega^2\left(I_{55} + \mu_{55}\right)\right] \end{aligned} \quad (3)$$

where C_{55} is the linear hydrostatic pitch spring coefficient, I_{55} is the OSWEC mass moment of inertia, and μ_{55} is the radiation-pitch-added moment of inertia.

The frequency-domain expression for the pitch-angular velocity response amplitude operator (RAO) can be calculated from

$$\frac{i\omega\xi_5}{A} = \frac{X_5}{\left[\lambda_{55} + \lambda_g\right] + i\left[-\left(C_{55} + C_g\right)/\omega + \omega\left(I_{55} + \mu_{55}\right)\right]} \quad (4)$$

where ξ_5 is the complex pitch displacement amplitude.

The structural foundation must handle the reaction force needed to fix the OSWEC to the seabed. The foundation force in surge, X_{r1}, is given by

$$A\left(X_{r1} + X_1\right) = \left[\lambda_{15} + i\omega\mu_{15}\right] i\omega\xi_5 \quad (5)$$

where X_1 is the complex surge wave-exciting force coefficient per unit wave amplitude, μ_{15} is the surge-pitch added mass, and λ_{15} is the surge-pitch wave radiation damping.

3.1 Nonideal PTO Units

As discussed in [10], reactive control [1] requires a two-way energy flow between the oscillating body and an energy storage system that will have losses associated with the energy flux reversal process. The effect of efficiency (η_e) on the output TAP was calculated in [10], which provides the following expressions

$$\begin{aligned} G &= \left|\frac{C_g}{\omega\lambda_g}\right| \quad \& \quad G^* = \arctan G \\ P_O &= \eta_e\frac{\lambda_g|i\omega\xi_5|^2}{2}\left(1 + e^* g^*\right), \ e^* = \frac{1-\eta_e^2}{\eta_e^2} \\ g^* &= \left(\frac{2G^* - \sin 2G^* - 2G\left(1 - \cos^2 G^*\right)}{2\pi}\right) \end{aligned} \quad (6)$$

where P_O is the TAP that is sent to the grid. To provide a measure of the capture efficiency for a given WEC, the TAP contained within a propagating wave must be known. The time-averaged wave-power-per-unit width (P_w) can be calculated from

$$P_w = \frac{1}{2}\rho g A^2 V_g = \frac{1}{4}\rho g A^2\sqrt{\frac{g}{k}\tanh kh}\left[1 + \frac{2kh}{\sinh 2kh}\right] \quad (7)$$

where V_g is the wave group velocity, k is the wave number, and g is the gravitational acceleration. The nondimensional capture width in this work will be defined

as

$$C_w = \frac{P_O}{wP_w} \tag{8}$$

where w is the OSWEC width.

4. PSEUDO-SPECTRAL CONTROL

The pitch angular velocity ($\dot{\zeta}_5$) and PTO control torque (τ_m) are approximated by a zero-mean truncated Fourier series [5] with N terms

$$\dot{\zeta}_5(t) \approx \sum_{j=1}^{N/2} \psi_j^c \cos(j\omega_0 t) + \psi_j^s \sin(j\omega_0 t) = \Phi(t)\,\hat{\psi} \tag{9}$$

$$\tau_m(t) \approx \sum_{j=1}^{N/2} \tau_j^c \cos(j\omega_0 t) + \tau_j^s \sin(j\omega_0 t) = \Phi(t)\,\hat{\tau} \tag{10}$$

$$\hat{\psi} = \left[\psi_1^c, \psi_1^s, \ldots, \psi_{\frac{N}{2}}^c, \psi_{\frac{N}{2}}^s\right]^\top \quad , \quad \hat{\tau} = \left[\tau_1^c, \tau_1^s, \ldots, \tau_{\frac{N}{2}}^c, \tau_{\frac{N}{2}}^s\right]^\top$$

$$\Phi(t) = \left[\cos(\omega_0 t), \sin(\omega_0 t), ..., \cos\left(\frac{N}{2}\omega_0 t\right), \sin\left(\frac{N}{2}\omega_0 t\right)\right]$$

with the fundamental frequency given by $\omega_0 = 2\pi/T$ and T being the chosen time duration. The pitch equation of motion can be described as follows

$$M_{55}\hat{\psi} = \hat{\tau} + \hat{e}_5 \tag{11}$$

where $\hat{e}_5$ represents the Fourier coefficients of the pitch wave-exciting torque. The matrix $M_{55} \in \mathbf{R}^{N\times N}$ is block diagonal with the following structure

$$M_{55}^j = \begin{bmatrix} \lambda_{55}(j\omega_0) & \alpha(j\omega_0) \\ -\alpha(j\omega_0) & \lambda_{55}(j\omega_0) \end{bmatrix} \quad , \quad \text{for} \quad j = 1, 2, \ldots, N/2$$

$$\alpha(j\omega_0) = j\omega_0\left(I_{55} + \mu_{55}(j\omega_0)\right) - C_{55}/(j\omega_0) \tag{12}$$

The pitch angular-velocity coefficients can be determined explicitly from the control and pitch wave-exciting torque Fourier coefficients. This representation allows the time-averaged absorbed power to be written as

$$\begin{aligned} P_T &= \frac{1}{T}\int_0^T \dot{\zeta}_5(t)\,\tau_m(t)\,dt = \frac{1}{2}\hat{\psi}^\top\hat{\tau} \\ &= \frac{1}{2}\left[\hat{\tau}^\top\left(M_{55}^{-1}\right)^\top\hat{\tau} + \hat{e}_5^\top\left(M_{55}^{-1}\right)^\top\hat{\tau}\right] \end{aligned} \tag{13}$$

which is in the form of a traditional quadratic problem. This representation does not account for the efficiency of nonideal PTO units; however, from this point forward, all results will have made corrections for PTO efficiency in postprocessing. The final objective function will be the sum of the time-averaged absorbed power, the squared ℓ^2-norm of the surge-foundation force (f_{r1}) and the control force magnitude. The three contributions will be nondimensionalized and combined as follows:

$$J = \frac{P_T}{wP_w} + \gamma\left|\underbrace{\frac{f_{r1}}{\frac{1}{2}\rho g w h A}}_{f_{r1}^*}\right|^2 + \beta_m\left|\underbrace{\frac{\tau_m}{\frac{1}{6}\rho g w h^2 A}}_{\tau_m^*}\right|^2 \tag{14}$$

5. REGULAR WAVE RESULTS

The PSC simulations were performed with a PTO efficiency of 85% and a maximum angular displacement

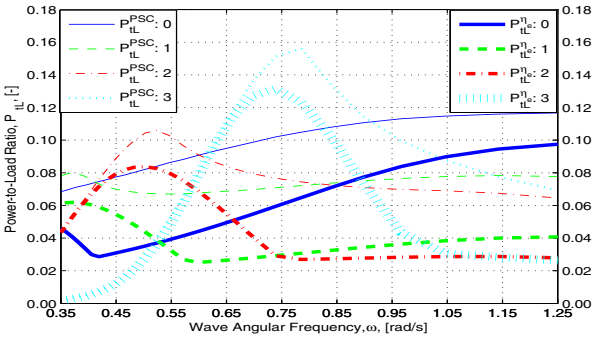

(a) Power-to-load Ratio

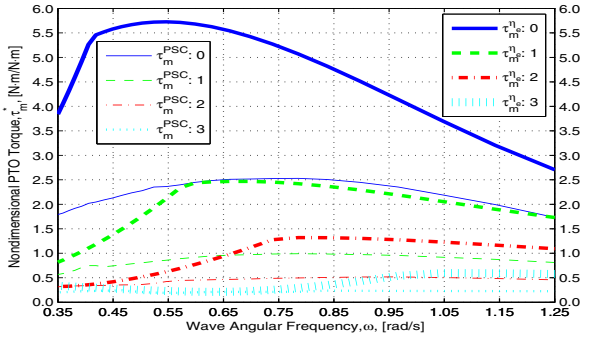

(b) PTO Control Torque

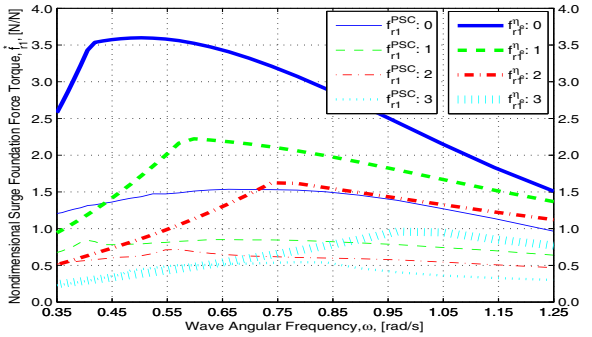

(c) Surge Foundation Force

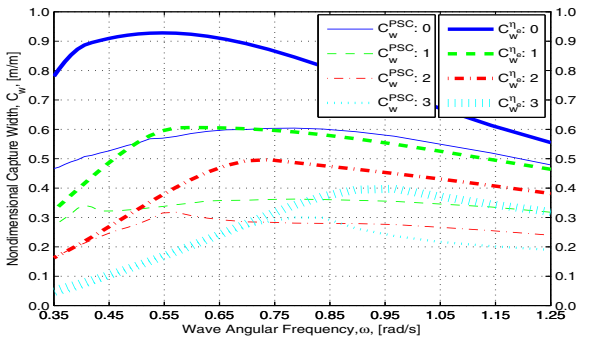

(d) Nondimensional Capture Width

Figure 3: Regular wave results for a wave amplitude of 0.5 m and varying wave frequency. The numbers in the legend denote the zero-flap, one-flap, two-flap, and three-flap open geometry. The superscript ^{PSC} denotes results from PSC which provide the optimum P_{tL} while $^{\eta_e}$ denotes results from maximizing the PTO output power given by Equation (6).

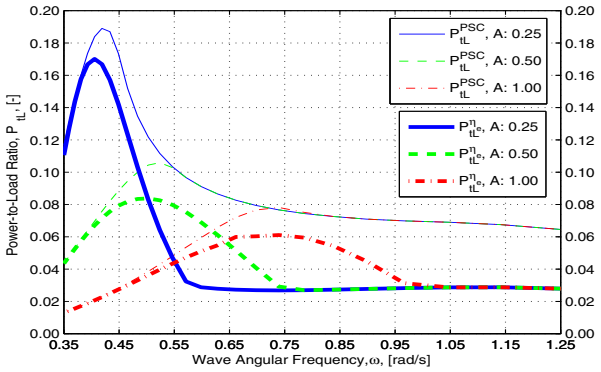

Figure 4: Power-to-Load ratio while varying the wave amplitude and frequency for the two-flap open configuration.

amplitude of $30^o(\pi/6)$. The following power-to-load ratio (P_{tL}) was constructed to evaluate OSWEC performance

$$P_{tL} = C_w \left(\frac{C_w}{f_{r1}^* + \tau_m^*}\right)\left(\frac{P_O}{\sigma_O}\right) \quad (15)$$

where σ_O is the standard deviation in the instantaneous output power. As this work considers only regular waves, in the calculation of P_{tL}, the values of f_{r1} and τ_m are taken as the peak values over the wave period. The first term in Equation 15 represents the net output power to the grid that is directly related to the annual energy production; however, the second term is included to temper the controller from allowing large structural loads, leading to greater steel thickness and higher capital costs. The third term was introduced to limit the PTO peak instantaneous power and control actuation effort, thereby minimizing the PTO power capacity requirements.

The maximum P_{tL} values obtained from applying PSC for combinations of the penalty weights (γ and β_m) have been plotted in Fig. 3(a). The results show that for all geometries and wave frequencies PSC produces P_{tL} values that are equal to or higher than when solely maximizing output power. With proper selection of the penalty weights used in the multiterm objective, we can obtain an increase in output power [see Fig. 3(d)] that exceeds the growth in structural loads [see Figs. 3(b) and 3(c)]. For the two-flap open geometry, the capture width has been reduced by only 40% compared to the maximum capture width whereas the structural loads have been reduced by approximately 60%. It can be observed that the maximum P_{tL} for each WEC geometry occurs near resonance when operating in low sea states. However, as the wave amplitude increases, the limit on the pitch displacement amplitude reduces the benefit of the amplified motion. As seen in Fig. 4, as the wave amplitude increases, the peak P_{tL} ratio decreases and shifts to higher wave frequencies. These preliminary results help demonstrate the benefit of combining a variable geometry WEC and PTO control to shift the operational focus between power maximization and load mitigation.

6. ACKNOWLEDGMENTS

This work was supported by the U.S. Department of Energy under Contract No. DE-AC36-08GO28308 with the National Renewable Energy Laboratory. Funding for the work was provided by NREL's Laboratory Directed Research and Development Program. The U.S. Government retains and the publisher, by accepting the article for publication, acknowledges that the U.S. Government retains a nonexclusive, paid-up, irrevocable, worldwide license to publish or reproduce the published form of this work, or allow others to do so, for U.S. Government purposes.

7. REFERENCES

[1] Falnes, J., 2002. Optimum control of oscillation of wave-energy converters. *International Journal of Offshore and Polar Engineering* 12 (2), 147–154.

[2] Babarit, A., Clément, A. H., 2006. Optimal latching control of a wave energy device in regular and irregular waves. *Applied Ocean Research* 28, 77–91.

[3] Eidsmoen, H., 1996. Optimum control of a floating wave-energy converter with restricted amplitude. *Journal of Offshore Mechanics and Arctic Engineering* 118 (2), 96–102.

[4] Cretel, J. A. M, Lightbody, G., Thomas, G. P., Lewis, A. W., 2011. Maximisation of energy capture by a wave-energy point absorber using model predictive control. In: 18th World Congress of the International Federation of Automatic Control, Milano, Italy, 3714–3721.

[5] Bacelli, G., Ringwood, J. V., 2015. Numerical optimal control of wave energy converters. *IEEE Transactions on Sustainable Energy* 6(2), 133–145.

[6] Zurkinden, A. S., Lambertsen, S. H., Damkilde, L., Gao, Z., Moan T., 2013. Fatigue analysis of a wave energy converter taking into account different control strategies. In: 32nd ASME International Conference on Ocean, Offshore, and Arctic Engineering, Nantes, France.

[7] Tom, N., Lawson, M. J., Yu, Y.-H., and Wright, A. D., 2016, Development of a nearshore oscillating surge wave energy converter with variable geometry. *Renewable Energy* 96, 410-424.

[8] Pecher, A., Kofoed, J. P., Espedal, J., Hagberg, S., 2010. Results of an experimental study of the Langlee wave energy converter. In: 20th International Offshore and Polar Engineering Conference, Beijing, China, 877–885.

[9] Evans, D. V., 1981. Maximum wave-power absorption under motion constraints. *Applied Ocean Research* 3(4), 200–203.

[10] Falcao, A. F. O., Henriques, J. C. C., 2015. Effect of non-ideal power take-off efficiency on performance of single- and two-body reactively controlled wave energy converters. *Journal of Ocean Engineering and Marine Energy* 1(3), 273–286.